




Article

UAV-Derived Data Application for Environmental Monitoring of the Coastal Area of Lake Sevan, Armenia with a Changing Water Level

Andrey Medvedev ^{1,2,*}, Natalia Telnova ^{1,2} , Natalia Alekseenko ^{1,2}, Alexander Koshkarev ¹ , Pyotr Kuznetchenko ¹, Shushanik Asmaryan ³  and Alexey Narykov ¹

¹ Institute of Geography, Russian Academy of Sciences; Staromonetny pereulok, 29, 119017 Moscow, Russia; telnova@igras.ru (N.T.); alekseenko@igras.ru (N.A.); koshkarev@igras.ru (A.K.); map@igras.ru (P.K.); narykov@igras.ru (A.N.)

² Faculty of Geography and Geoinformation Technology, National Research University “Higher School of Economics”, Myasnitskaya Ulitsa 20, 101100 Moscow, Russia

³ Centre for Ecological-Noosphere Studies, National Academy of Sciences, Abovyan Street 68, Yerevan 0025, Armenia; shushanik.asmaryan@cens.am

* Correspondence: medvedev@igras.ru; Tel.: +7495-959-38-49

Received: 29 September 2020; Accepted: 18 November 2020; Published: 21 November 2020



Abstract: The paper presents the range and applications of thematic tasks for ultra-high spatial resolution data from small unmanned aerial vehicles (UAVs) in the integral system of environmental multi-platform and multi-scaled monitoring of Lake Sevan, which is one of the greatest freshwater lakes in Eurasia. From the 1930s, it had been subjected to human-driven changing of the water level with associated and currently exacerbated environmental issues. We elaborated the specific techniques of optical and thermal surveys for the different coastal sites and phenomena in study. UAV-derived optical imagery and thermal stream were processed by a Structure-from-Motion algorithm to create digital surface models (DSMs) and ortho-imagery for several key sites. UAV imagery were used as additional sources of detailed spatial data under large-scale mapping of current land-use and point sources of water pollution in the coastal zone, and a main data source on environmental violations, especially sewage discharge or illegal landfills. The revealed present-day coastal types were mapped at a large scale, and the net changes of shoreline position and rates of shore erosion were calculated on multi-temporal UAV data using modified Hausdorff’s distance. Based on highly-detailed DSMs, we revealed the areas and objects at risk of flooding under the projected water level rise to 1903.5 m along the west coasts of Minor Sevan being the most popular recreational area. We indicated that the structural and environmental state of marsh coasts and coastal wetlands as potential sources of lake eutrophication and associated algal blooms could be more efficiently studied under thermal UAV surveys than optical ones. We proposed to consider UAV surveys as a necessary intermediary between ground data and satellite imagery with different spatial resolutions for the complex environmental monitoring of the coastal area and water body of Lake Sevan as a whole.

Keywords: UAV; highly-detailed spatial data; thermal survey; coastal processes; shoreline position; coastal wetlands; eutrophication; multi-platform environmental monitoring

1. Introduction

1.1. Overview of Current Thematic Applications of Unmanned Aerial Vehicles (UAV) Surveys in Coastal Environments

The last decade has seen rapidly increasing interest in a large range of thematic applications for ultra-high spatial resolution data derived from small, low-cost, unmanned aerial vehicles (UAVs) as an essential component for remote sensing monitoring in coastal environments [1–3]. UAV-based remote sensing is also considered a rather simple and easily replicable tool for environmental coastal monitoring even for non-experts in specific surveying technologies and processing of derived data [4]. The clear advantages of this approach are cost-effectiveness and flexibility. Provision of data with very high spatial (sub-centimeters) and temporal (on demand and simultaneously with field measurements) resolutions allows reliable identification of specific objects and processes in highly dynamic conditions and areas at risk of human or natural-induced degradation [1,5,6]. Currently, operational and prospective thematic applications of UAV-derived data in environmental remote sensing monitoring and management of coastal marine, lacustrine, and riverine areas with high anthropogenic impacts are very diverse. Among them there are such issues as: (a) short-term and long-term dynamics of shorelines [7–10], (b) reconstruction of submerged topography in shallow waters [11], (c) high-resolution surveys of coastal morphology and hazardous processes [12–14], (d) delimitation and large-scale mapping of nearshore aquatic and intertidal ecosystems [15–18], estuarine habitats [19], and coastal wetlands [20,21]. Within the sphere of coastal management, one very novel and specific application of UAVs is the monitoring of littering, resulting from recreational activities, as well as of nearshore marine and lacustrine waters and adjacent coasts with high and diverse anthropogenic impacts [22–24].

Since many marine coastal waters and inland freshwaters worldwide are now exposed to severe water quality issues connected with persistent outbreaks of harmful algal blooms (HABs) due to anthropogenic eutrophication [25], UAV-based monitoring of HABs and sources of water pollution is now considered a very promising and powerful tool [2,26,27]. UAV-derived water quality data with high spatial resolution are the most appropriate for smaller lakes, reservoirs, irrigation ponds, and riverine and coastal waters, which often have high anthropogenic loads but are not properly recognizable at the spatial resolutions of existing satellite sensors [5]. The significance of UAV-based monitoring of water quality and distribution of algal blooms as a part of an “early warning” remote sensing system is clearly demonstrated in References [6,27].

As a whole, UAV surveys can now be considered a necessary intermediary between in situ measurements and satellite remote sensing for integral multi-temporal and multi-scale environmental monitoring of coastal areas [27]. Consequently, the elaboration and realization of an appropriate protocol on the collection, and processing of UAV data, by taking into consideration both the possibilities and limitation of surveys in defined areas, are rather urgent study tasks [28,29].

1.2. Study Objectives Associated with Environmental Issues of Lake Sevan when Changing Its Water Level

Lake Sevan, as Armenia's largest freshwater resource, is of vital importance not only nationally but throughout the South Caucasus region. Being of great significance to irrigation, fisheries, hydropower, recreation, and tourism, as well as to sustaining valuable freshwater, associated populations, and endemic species, Lake Sevan has been subjected to a complex set of environmental issues since the early 1930s, when the water level was significantly dropped due to extensive water withdrawal for irrigation (Figure 1).

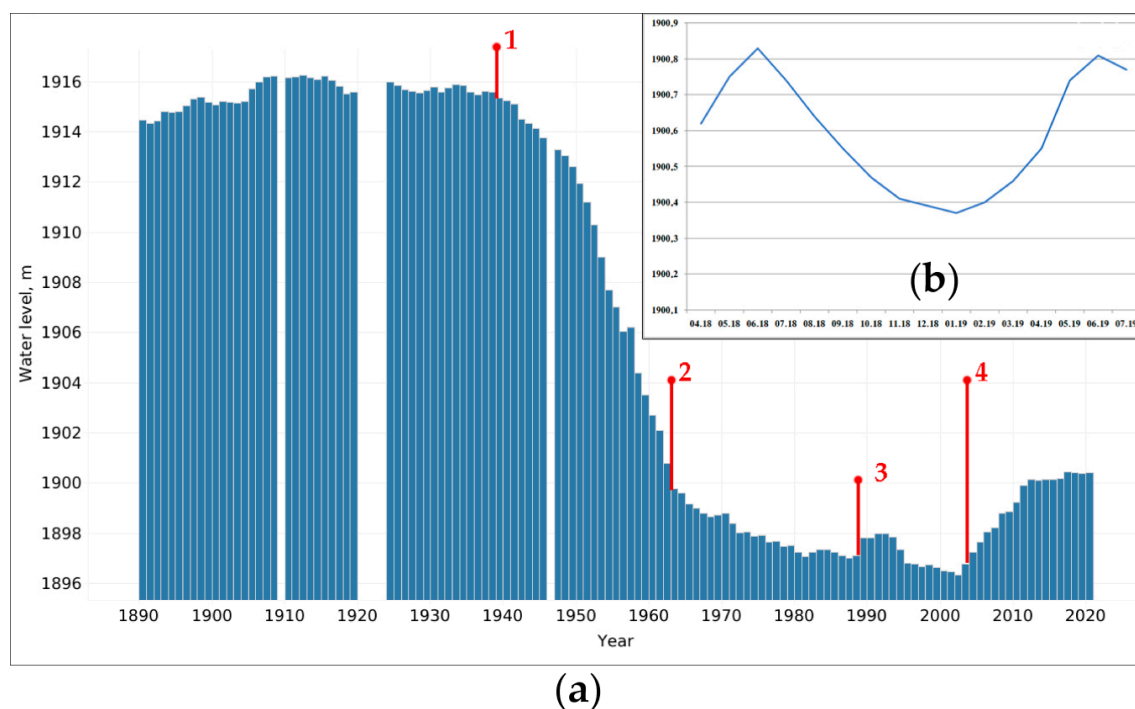


Figure 1. (a) Annual changes in Lake Sevan water level from 1890 to 2020. (b) Monthly changes in water level during unmanned aerial vehicle (UAV) surveys, April 2018–July 2019. Red lines and figures mark the following events: 1–the start of artificial drop of the water level, 2–the decrease of water withdrawal on irrigation purposes, 3–Arpa-Sevan tunnel is fully operational (inflow of 200 mln. m^3 of water annually), 4–Vorotan-Arpa tunnel is operational (additional water inflow of 165 mln. m^3). Credits: data from 1890 to 1920 [30], from 1927 to 1998 [31], from 2002 to 2016 [32], and then according to data from the Ministry of Emergency Situations, Republic of Armenia [33].

In the 2000s, the Republic of Armenia enacted the “Law on Lake Sevan” and “Law on Measures for Restoration, Maintenance, Reproduction, and Use of Lake Sevan Ecosystem” (2001) [34] and a spatial planning project for the Lake Sevan drainage basin (2003) [35]. These laws refer to plans for raising the water level by 6 m up to the optimal altitude of 1903.5 m by the year 2030. Taking into account the current inflow and withdrawal, this means a raise of the water level by 21.6 cm annually [34]. However, the rapidly raised water level has led to serious issues of shore submergence and flooding of the built-up coastal zone. In 2011, it was officially approved to limit the increase in the lake water level [36]. Such long-term and short-term changes in the water level of Lake Sevan have caused drastic transformations in coastal and aquatic ecosystems as well as the limnological and hydro-chemical properties of lake waters [37–39]. The first algal bloom in Lake Sevan was observed in 1964, and, since 2018, repeated summer outbreaks of *Cyanophyta*, have encompassed the whole lake area and are clearly classified as toxic [40]. The coastal zone and the entire Lake Sevan’s basin area are now subject to anthropogenic impacts that are large in extent and diverse in type. This, combined with ineffective environmental management and regulation measures, exacerbates the state of coastal and water environments, which are also vulnerable to climatic changes and seismic events [41].

Nevertheless, in spatial and temporal terms, there is a little knowledge about factors and drivers of negative impacts and coastal ecosystem responses to them. Enacted measures of water, agricultural, and environmental policies are not well balanced in Sevan Basin [36,42]. There is a low public awareness on all the aspects of environmental responsibility, resource use, and ecosystem services provided by Lake Sevan. Under such conditions, there is evidently a need to devise and implement a remote sensing system for regular monitoring of the coastal environments and rapid response to their changes based on such a flexible and operative tool as UAV surveys. Taking into account the very complex set of environmental issues and their intricate spatio-temporal patterns, the present study

examines the possibilities, specific features, and applications of UAV-based environmental monitoring of Lake Sevan's coastal zone as an initial and important elaboration stage of multi-platform, multi-scale, and multi-temporal remote sensing scheme for monitoring this highly dynamic and vulnerable area. In this paper, we focus on several topical thematic applications based on optical and thermal UAV imagery. Such thematic tasks as identification and large-scale mapping of point and non-point sources of lake eutrophication and algal blooms can be resolved only by means of a multi-platform and a multi-scale approach, where UAV-derived imagery need to be supplemented by satellite multispectral data. The other objective is a highly-detailed assessment of present-day coastal processes based on multi-temporal UAV data. The current state of vulnerable coastal wetlands and marsh coasts was studied from light-weight UAV using several surveying and data processing techniques to highlight the advantages of coastal monitoring with thermal, highly detailed imagery. We also detected and mapped the coastal habitats, buildings, and facilities at a large scale under the risk of submerging in case of intended raise of the water level up to 1903.5 m. Approaches and findings of such UAV-based monitoring can be valuable for coastal environments and environmental management of large lakes or water reservoirs in mountainous regions not provided with up-to-date and detailed spatial data.

2. Materials and Methods

2.1. Study Site

Lake Sevan ($40^{\circ}23'N$, $45^{\circ}21'E$) is a high-altitude lake located approximately 1900 m above sea level in the Gegharkunik province of Armenia. It is one of the largest lakes in the entire South Caucasus region and one of the largest freshwater high-mountain lakes in Eurasia with a maximum length and width of approximately 70 km and 50 km, respectively. Morphologically, Lake Sevan is divided into two basins, the Major and Minor Sevan, which differ in their time of formation, origin, and average depth. According to data from 1 January 2017 [32], the total lake surface area is 1278.6 km² with a mean depth above 26 m. Surface areas of deeper Minor Sevan and a shallower Major Sevan are 338.6 and 950.0 km², respectively [32]. Lake Sevan drainage basin now covers 4721 km² [42]. The lake is fed by 28 rivers and drained by the Hrazdan River, which originates at the northwest extremity of the lake. The main inflow sources of the lake are river waters, water inflow from the Vorotan–Arpa and Arpa–Sevan tunnels, and groundwater inflow. Main outflow components are the Hrazdan River, evaporation from the lake surface, water discharges, and groundwater outflow. According to the Ministry of Emergency Situations of the Republic of Armenia, the water level altitude was 1900.43 m by 1 January 2020, and had increased to 1900.73 m by 11 August 2020 [33].

We determined the coastal zone boundaries according to the natural shoreline of Lake Sevan, as reconstructed from historical small-scales bathymetric maps from 1929, i.e., before the long and dramatic human-induced drop of the lake water level. Several key sites in this area that display the most pronounced changes in shoreline since the 1930s reflect diversity of coastal types (in terms of their geomorphometry and prevailing processes) and current land-use patterns were chosen for repeated UAV-based surveys (Figure 2). It should be noted that the number of sites was limited due to legislative restrictions concerning UAV surveys in some areas (the mouth of Martuni River).

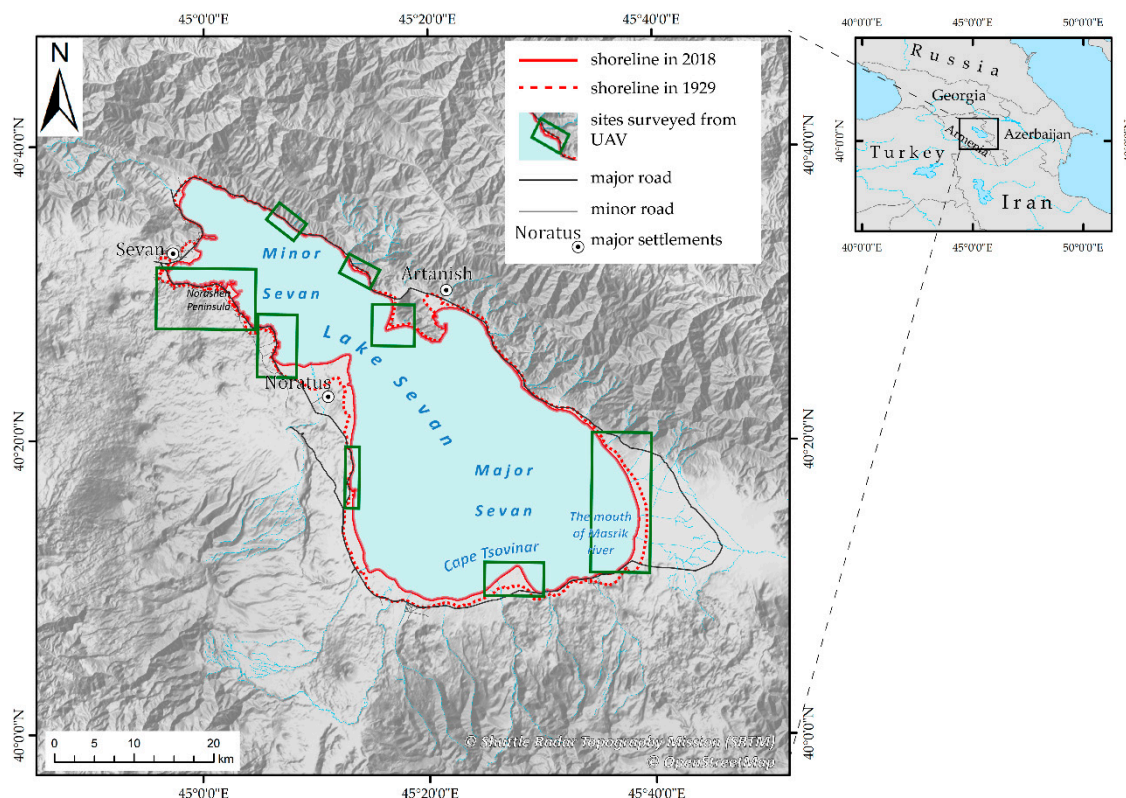


Figure 2. Study site location and sites of repeated UAV surveys in 2018–2019.

2.2. Mapping of Land Use and Present-Day Shoreline on a Basis of Satellite and UAV Imagery

Seamless mosaics of very high-resolution imagery provided via web-services Yandex.Maps, GoogleMaps, BingMaps (Microsoft), and ArcGIS.Imagery (ESRI) were used as data sources at the first stage of study for large-scale thematic mapping of the coastal zone. These mosaics were interpreted visually for recognition of buildings and land use large-scale mapping in the coastal zone. The following principal types of present-day land use were identified in coastal zone: man-made forests and shrublands, natural pastures (flood plain meadows and grasslands), coastal wetlands, residential built-up areas, industrial units, recreational facilities, arable lands, bare lands disturbed by human activities such as mining exploration and dumping sites, and road network. Key sites mapped in the course of UAV surveys and simultaneous field observations were used as a reference and ground data for interpretation of land cover and land use types. We also identified and mapped detached buildings in the coastal zone and livestock farms as objects under the risk of submerging in case of water level rising, potentially having adverse impacts on the ecological state of lacustrine waters as point sources of sewages.

Additionally, we employed multi-seasonal and multi-spectral satellite data from Landsat 8 Operational Land Imager (OLI) to detect contemporary land cover and land use pattern throughout the entire drainage basin. From Landsat 8 Collection of Level 1 processing products (Courtesy of U.S. Geological Survey), we choose three scenes with different acquisition date of 2019: 15 May, 2 July, and 20 September. We converted digital numbers to the reflectance values at the top-of-atmosphere reflectance in red, near-infrared (NIR), and shortwave-infrared spectral bands. Then, we performed supervised classification of these multi-seasonal and multi-temporal data through a Support Vector Machine (SVM) algorithm in SAGA (System of Automated Geoscientific Analyses) GIS open source GIS software. Training and testing samples for nine general land cover classes were randomly chosen from ground data, high resolution satellite, and UAV imagery. As a result, the spatial distribution of nine land cover classes (built-up areas, arable lands, dry and alpine mountainous grasslands,

natural meadows, shrublands, forests, bare areas, and water) was acquired and analyzed for the whole area of the Lake Sevan drainage basin.

Seamless mosaics of highly detailed satellite imagery acquired via web-services Yandex.Maps, GoogleMaps, BingMaps (Microsoft), and ArcGIS.Imagery (ESRI) were also used for mapping coastal types along the whole shoreline of Lake Sevan. The classification of present-day coastal types was verified by UAV surveys and ground truth data (reference points) along the entire lake shore. Ground surveys enabled identification of beach processes being active at specific locations, while UAV-derived ortho-imagery enabled the extrapolation of identified characteristics to other areas by inter-comparison of interpretation parameters.

2.3. UAV-Based Optical Survey for Detection of Coastal Processes and Phenomena

The optical survey techniques used within the study methodology can be divided into several tasks: mapping of the shoreline, constructing a digital surface model (DSM) for modeling the shoreline position, land use mapping, and pollution monitoring of water areas and coasts. Aerial photography was performed from the small UAV DJI Phantom PRO. According to the different study tasks, flight levels for the surveys were 100, 200, and 400 m above the surface (Table 1). Most extensive and long surveys were performed at 400 m elevation, while human-induced disturbances and shoreline fluctuations were detected from a height of 100 m.

Table 1. Survey techniques and features of UAV-derived data according to thematic study tasks.

Flight Altitude, m		Thematic Tasks	Overlap of Acquired Imagery, %	Mean Spatial Resolution of Orthomosaics, cm	Mean DEM's and DSM's Spatial Resolution, cm	Mean Point Density in Dense Point Clouds, Points Per sq. Meters (Water/Ground)
100	RGB	detection of shoreline positions, monitoring of pollution and littering.	80	3.1	6.2	97/311
200	RGB	monitoring of coastal waters' pollution, constructing DSM, modeling of shoreline position	80	6.4	12.8	63/137
400	RGB	land use mapping, constructing DSM.	90	12.7	25.4	11/29
	Thermal	detection of the shoreline positions and wetlands structure, identification of water mixing, decay of submerged vegetation	80	47.3	94.6	6/13

Photogrammetric processing of optical survey data was performed in Agisoft MetaShape using a Structure-from-Motion (SfM) technique for imagery conversion into 3D models. The software includes a standard processing flowchart with aligning photos, dense point cloud generation, and building of models [43]. According to survey flight levels, the resulting DSM spatial resolution ranges from 6.2 to 25.4 cm. DSMs were then used to produce various parameters for the coastal zone, classification of coastal types, and determining shoreline position.

Visual interpretation of UAV-based optical ortho-imagery (in three visible bands -Red, -Green, Blue, or RGB) with spatial resolution from 3.1 to 12.7 cm was performed on a basis of direct distinguishing features as detected objects (such as garbage, landfills, wastewater discharge points, and other sources of environmental problems) can be well identified only on images with a spatial resolution of the first decimeters or higher (Figure 3).

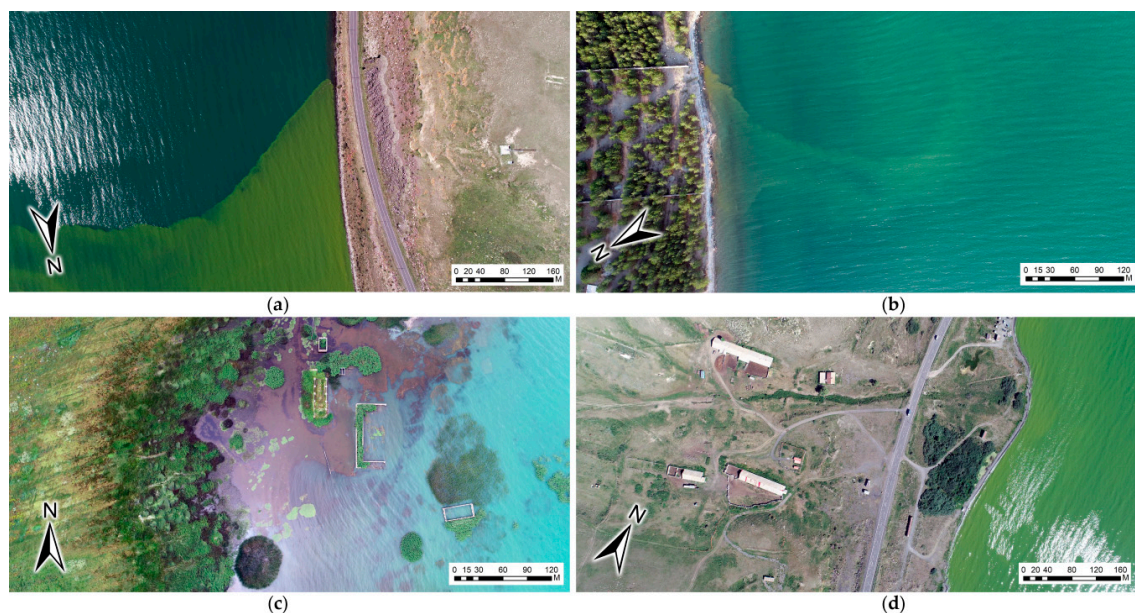


Figure 3. Point sources of pollution and processes in Lake Sevan coastal waters detected from UAV surveys in July 2019: (a) *Cyanophyta* outbreaks, (b) sewage discharge from a recreational facility, (c) submerging of coastal buildings, and (d) a small livestock farm near the shores.

At the stage of flight-planning, we also conducted a spatial analysis of water quality in terms of turbidity and algal blooms using satellite imagery from PlanetScope constellation. These multi-spectral data are acquired up to several times per day at a spatial resolution of 3 m, and free access to the data was granted under an individual research license [44]. We utilized surface reflectance products [45] to create short-term consistent time series of such a spectral index as a Surface Algal Bloom Index (SABI). SABI is a robust four-band index for detecting areas with high primary production of surface phytoplankton during the period of algal blooms [46]. SABI was calculated according to Equation (1).

$$\text{SABI} = (\text{NIR} - \text{Red}) / (\text{Green} + \text{Blue}), \quad (1)$$

where NIR, Red, Green, Blue—spectral surface reflectance in appropriate channels of PlanetScope imagery.

It should be noted that meteorological conditions differed greatly during our UAV surveys at various coastal sites with major effects on water transparency. Thus, automated shoreline detection by DSM or orthomosaics was not feasible for all the locations. At the sites with standing waters and without surface waves, most data processing results also concerned shallow water bathymetry. Consequently, most of our work on detecting shoreline position utilized visual interpretation. UAV surveys of shoreline and coastal zone were performed in the course of fieldwork during 2018–2019 at different

daylight hours. Features such as wind ripples, flecks, and water glints introduced nuances into the survey and data processing techniques. In particular, they made it necessary to carry out an expert review and additional verification of data processing results under a small quantity of aligning points between images for the water surface. This challenge generally results to lower density of formed point clouds for surveyed water surfaces when compared to the ground (see the right column in Table 1).

2.4. Thermal Survey of the Coastal Zone

Thermal UAV surveys of two key study sites (Norashen Peninsula and the mouth of Masrik River, see Figure 2) were performed to enable more accurate detection of the shoreline position, recording processes of submerged vegetation decay, and detection of spatial patterns and interfusion processes of waters characterized by different temperature gradients (influx of rivers into the lake, water bodies of lagoons and backwaters).

DJI Phantom 4 UAV was used with an integrated thermal camera (FLIR BOSON) providing thermal video imagery within the spectral range of 7.5–13.5 μm . The survey was performed during predawn hours at two flight levels of 300 and 400 m above the surface. The survey route was planned so that the overlap of adjacent traverses reaches 80% and includes obligatory flights over key sites having maximal temperature gradients due to diversity and contrast of land cover types.

Modern thermal cameras used on UAVs are bolometers and have their own peculiarities in terms of brightness temperatures registration [47,48]. They typically show dependence between registered brightness values and camera-to-subject distance. Furthermore, data quality and processing algorithms are significantly affected by camera distortion responsible for the effect of a temperature difference between the center and («colder») edges of a frame. This effect diminishes frame-overlap, and automated algorithm of matching and aligning frames cannot be used because of very low quality of reciprocal orientation of frames and high noise levels in the resulting data.

When using a digital photogrammetric system (DPS) with UAV-based thermal aerial photography data, the processing technique is essentially similar to that used for optical aerial imagery [49,50] with the addition of stages required for processing the video stream recorded by thermal cameras. More accurate camera calibration is also necessary. Nevertheless, the peculiarities of UAV-based thermal aerial photography data often preclude the use of automated procedures provided by standard packages. Instead, some operations (e.g., positioning of matching points) must be performed manually because certain objects have different temperature gradients in terms of recognition, which is variable from the survey beginning to its end.

The processing algorithm of thermal survey data, performed in Agisoft MetaShape software, included the stages presented in Figure 4. Video record frames were converted into a set of images in increments of 20 frames. Under the camera, calibration utilized values of the camera parameter input were set as a matrix pixel size of 0.012×0.012 mm and a focal distance of 4.3 mm.

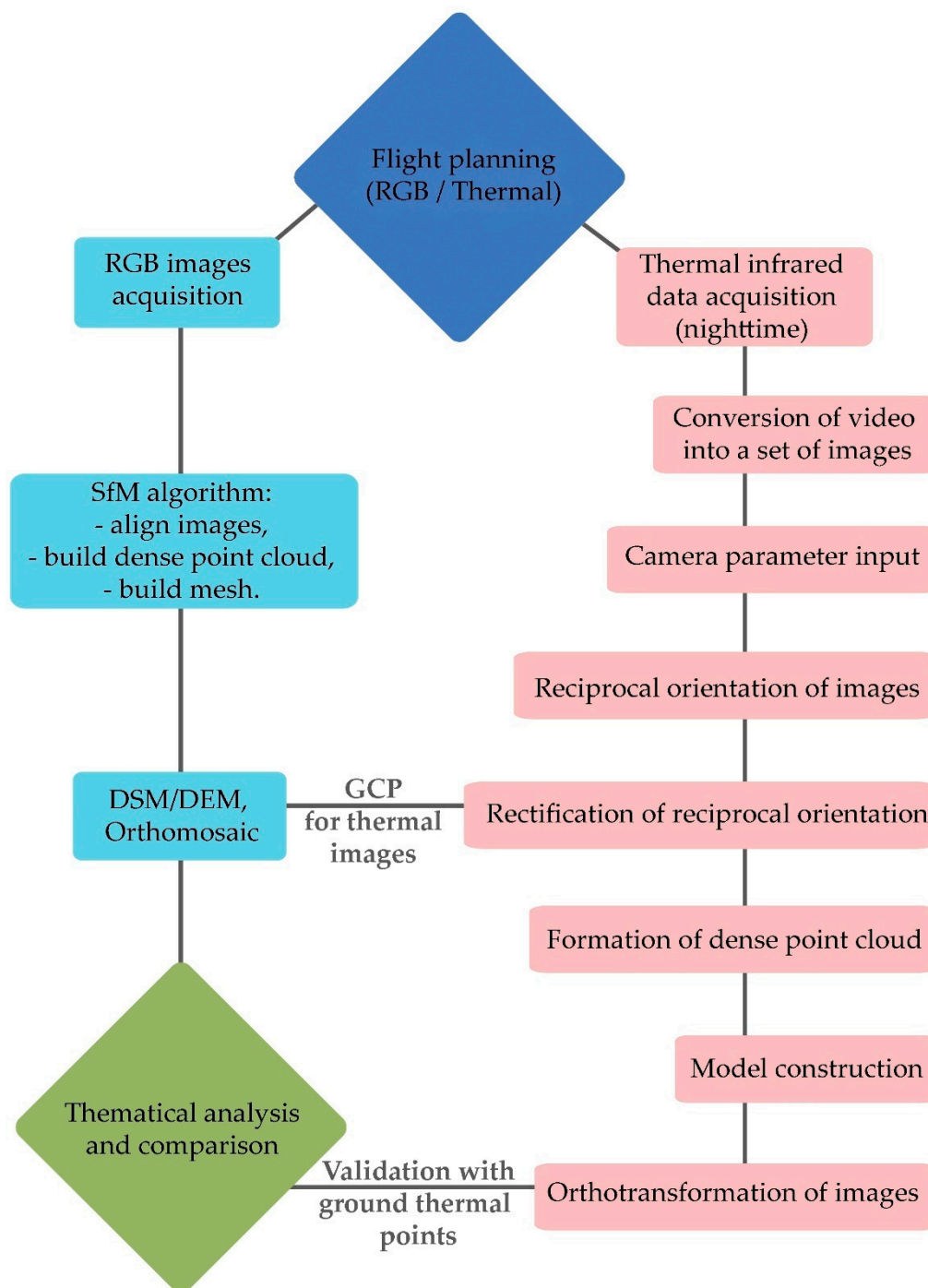


Figure 4. The processing flowchart of UAV-derived optical (RGB) imagery and thermal video stream.

The final ortho-mosaic is a rasterized image of brightness values with a radiometric resolution of 8 bit (256 scale units per pixel). This information cannot be directly interpreted as a temperature without terrestrial sensor calibration. In order to calibrate and classify thermal survey data as brightness temperature, several specific objects with maximal temperature value gradients should be chosen. In the course of UAV flights, these objects are surveyed at fixed intervals to determine the main regularities of the temperature change during different time periods.

2.5. Determining Rates of Shore Erosion and Shoreline Location Modeling

In order to determine the net changes of shoreline and annual rates of shore erosion, the shoreline location was specified using ortho-mosaic compiled from UAV-based surveys during 2018 to 2019. Multi-temporal ortho-mosaics were manually co-registered to align each other with one-to-one-pixel accuracy. Ground control points (GCPs) were set as unchanged objects in the coastal zone such as large stones, notable trees, road crossings, or artificially-coloured ground markers.

The shoreline positions on different dates were evaluated using modified Hausdorff distance as a measure of distance between two trajectories. This technique is widely used in geographical research for assessing distances between two complex linear objects [51,52]. Modified Hausdorff distances were calculated in ArcGIS Model Builder using an algorithm based on successive calculation of the shortest distances between shoreline positions. Additionally, a transition matrix was constructed of calculated distances between shoreline positions on different dates. As a result, the attribute table of modified Hausdorff distances also includes information specifying the type of coasts for each distance.

Shoreline position modeling within the framework of Roadmap for Lake Water Level Raising [34] was performed using DSMs compiled from UAV-based surveys. Since the shoreline positions show intra-annual movements, we modeled them in increments of 10 cm. Modeling was performed using a Water Rise Calculation Tool in Global Mapper software. The modeling results enabled identification of flooding zones and assessment of the size of built-up areas at risk of submerging and waterlogging.

3. Results

3.1. Point and Non-Point Sources of Anthropogenic Impacts on Coastal Lands and Waters

Since water discharge from Lake Sevan is regulated artificially, water level fluctuations are determined not only by seasonal hydroclimatic changes and extremes but also by the needs of various water users. Anthropogenic point-source effluents and non-point agricultural runoff within the coastal zone and the entire Lake Sevan drainage basin can be regarded as the main causes of lake water eutrophication and factors in increased frequency and intensity of hazardous algal blooms. Consequently, most environmental monitoring tasks involve examining the environmental impacts of recreation and other economic activities within the coastal zone and the Lake Sevan drainage basin.

Within the entire drainage basin, such land cover classes as built-up areas, arable lands, grassland, and meadows (often used for livestock), which can be considered as potential disperse sources of lake eutrophication [25]. The distribution of settlements, roads, and agricultural lands obtained as a result of land cover classification of Landsat 8 imagery is presented in Figure 5a. For the purposes of determining human-induced impacts on coastal environments and detecting potential sources of water pollution, large-scale maps of present-day land use and density of buildings in the coastal zone were compiled (Figure 5b,c). These maps display that the coastal zone of Lake Sevan is characterized by a diversity of present-day land use types with the following spatial patterns. Areas with recreational facilities and developed recreational infrastructure are concentrated along the shores of Minor Sevan, while natural pastures and forests are common along the shores of Major Sevan (Figure 5b). Just within the coastal zone, small patches of non-irrigated arable lands and vegetable gardens are generally adjacent to many villages and the small town of Sevan. Both in the coastal zone and within the entire drainage basin, steppe, and meadow pastures as well as small livestock farms are most widely represented. The main areas of irrigated and non-irrigated croplands are situated in the Masrik floodplain and along the fertile debris cones from the Sevan Mountain Ridge. These are important non-point sources of phosphorus-rich and nitrogen-rich runoff in the southeastern part of the Major Sevan. Areas of forest that were planted on drained lands in the 1960s and 1970s are now highly fragmented and partially replaced by secondary small tree and shrub vegetation. Our field observations and UAV data of 2018–2019 testify present-day disturbance of these man-made pine and deciduous forests by intensive pasturing and uncontrolled recreation (see images in Figures 2 and 6). For some coastal sites,

forest stand degradation is caused by contemporary flooding processes (northern shore of the Noratus Peninsula) and intensive erosion of shores (Cape Tsovinar).

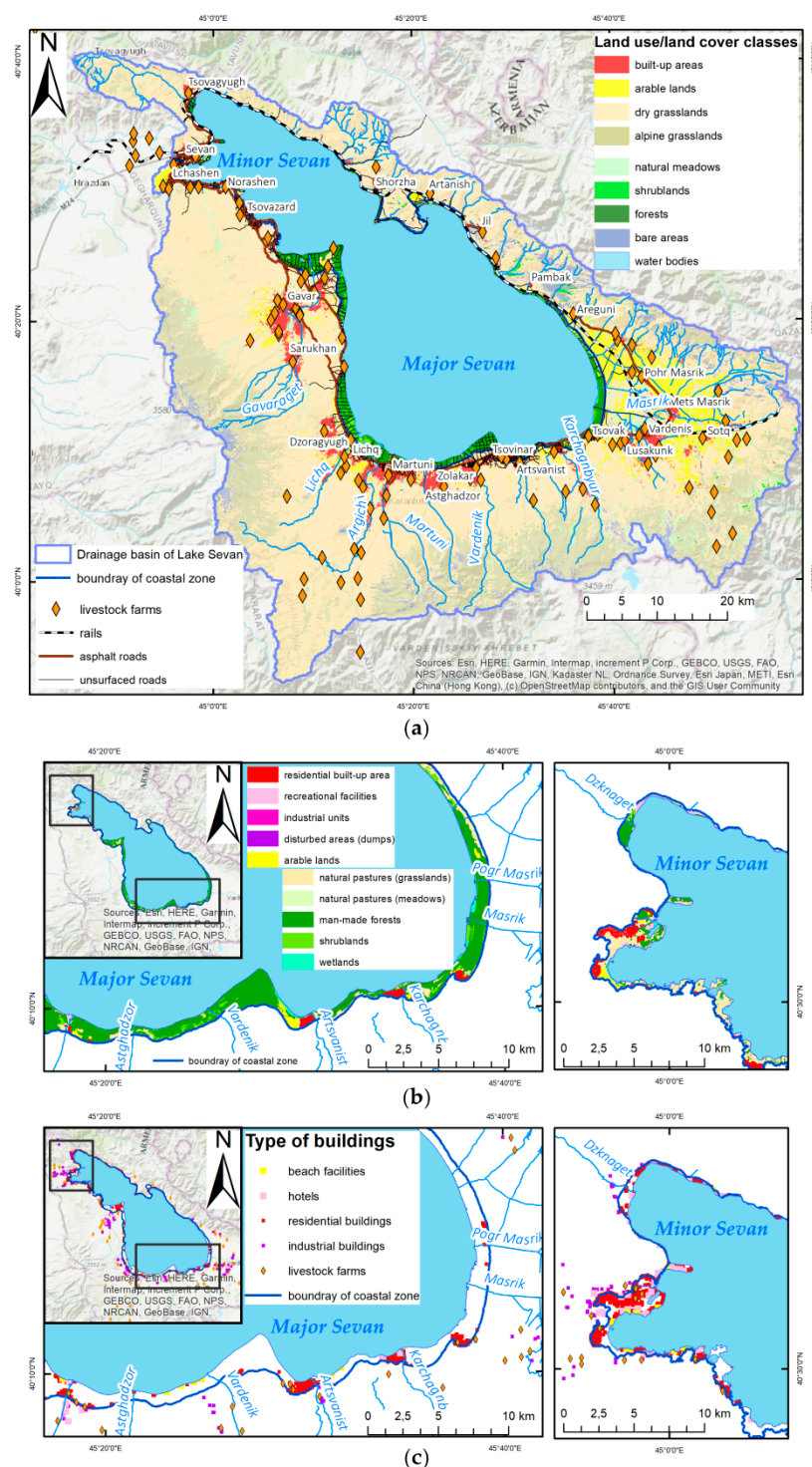


Figure 5. Point and non-point sources of anthropogenic impacts on coastal lands and waters: (a) Arable lands and livestock farms in the drainage basin of Lake Sevan. (b) Current land-use structure in the coastal zone. (c) Density of buildings in the coastal zone.

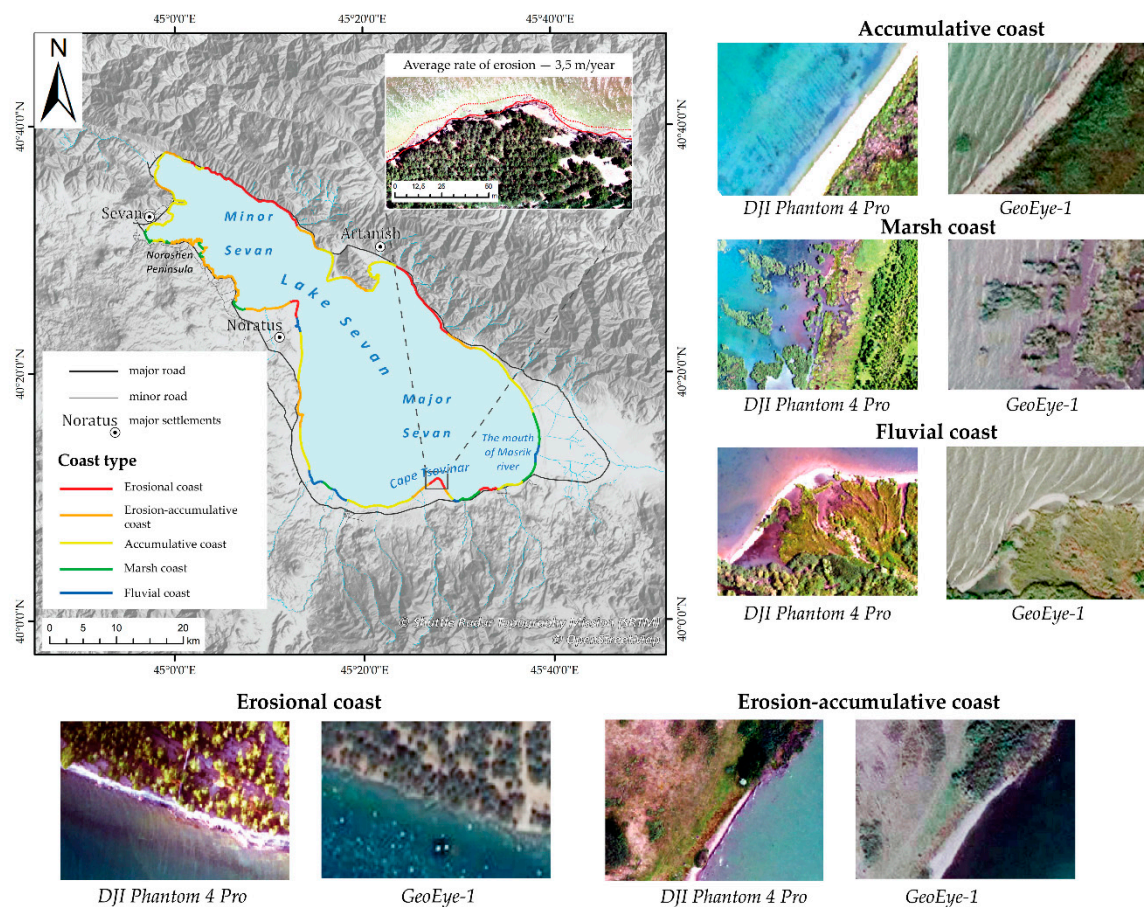


Figure 6. Present-day coastal types along the Lake Sevan shoreline.

Overall, residential and recreational built-up areas make up 15% of the coastal zone. UAV-derived highly detailed orthomosaic provide information on the numbers of various building types (residential houses in urban and rural settlements, single buildings of recreational purpose, livestock farms, industrial units) and their status (operational or abandoned).

Residential buildings are distributed along the shore unevenly due to topography. The very steep slopes of the Areguni Mountain Ridge break down to narrow beaches and cliffs along the northeast shoreline. Large rural settlements and the only small town (Sevan) are situated along on the western and southern shores. Visual interpretation of highly-detailed imagery identified 3002 residential buildings with a different number of stories in Sevan town, and about 2000 buildings in rural settlements. Their total distribution within the coastal zones of both Major Sevan and Minor Sevan is approximately the same (around 1000). In coastal zones, there are also many single isolated buildings (904), but they are 4.5 times less abundant along the Major Sevan than the Minor Sevan. Differences in the numbers of recreational facilities (primarily hotels) are also related to topography with their predominance along the western shores of Minor Sevan (Figure 5c). There is one-third the number of hotels located on the Major Sevan than on the Minor Sevan (total 68).

There are 25 temporary beach constructions, which are also concentrated at the Minor Sevan and, to a lesser degree, along the western shores of the Major Sevan. The southern shores are flatter and more marshy or waterlogged, and do not experience high pressure from organized recreation, accounting for only eight hotels and seven beach constructions. However, most coastal livestock farms (above 120 one) occur mainly along the shores of Major Sevan.

3.2. Coastal Types and Processes

Monitoring of shoreline and beach processes as well as comprehensive environmental monitoring of the coastal zone is often associated with the use of various remote sensing (RS) platforms [27,53]. Some problems emerge in the course of monitoring rapid coastal processes when situations change quickly due to hydrometeorological conditions, dynamic properties of objects, and phenomena themselves. In those cases, there is an issue to acquire simultaneous or repeated RS data with high spatial resolution from existing satellite platforms.

In the course of our UAV surveys, the shoreline position was primarily detected (at 84.4 km along the entire Lake Sevan coasts) because the slightest changes can trigger a chain of negative processes influencing the state of lacustrine environments. Changing the water level in Lake Sevan continues to entail significant transformations of limnological and hydro-ecological parameters, especially trophic status, the structures of coastal wetland, and aquatic ecosystems [37–39]. Changes in rate and type of coastal processes (erosion, waterlogging, and flooding) lead to the rapid degradation of coastal habitats and formation of dead biomass, thus, creating favorable conditions for phytoplankton development [39].

Based on collected field data in 2018–2019 (UAV-derived aerial imagery, terrestrial photography of reference points and field observations sites), combined with GeoEye-1 image (2017), present-day coastal types were identified and mapped at a large scale. Coastal types were determined in accordance with two classification schemes developed by Russian geomorphologists [54,55]. Classification based on shore genesis [54] allows specifying the presumed genesis of shores in their initial state. The shores developed under wave effects can be divided in three coastal types by currently dominating shore processes [55]. Present-day coastal types of the Lake Sevan and their relative distribution are presented in Figure 6 and Table 2.

Table 2. Present-day coastal types and their distribution by length along the Lake Sevan shoreline.

Coastal Types by Genesis and Dominating Processes		Length of the Total Coastline, %
developed under wave effect	accumulative coasts	38.6
	erosional coasts	28.1
	coasts with active shore erosion and accumulation	17.8
developed under the effect of biogenous factors	marsh coasts	10.1
developed under the effect of permanent stream accumulation	fluvial coasts	5.4

Erosional coasts of the Norashen and Tsovinar peninsulas, which are under the effect of active transformation, as well as the shores developed under the effect of permanent stream accumulation of the Masrik River, were surveyed repeatedly in 2018–2019 every six months to more accurately determine the dominant coastal processes by comparison of shoreline positions. Our modified Hausdorff distance calculations for the key coastal sites show that the net changes in the shoreline position for erosional cliffs of the Tsovinar between September 2018 and July 2019 were -2.91 m on average, giving the annual rate of shore retreat as 3.65 m with a standard error of 0.87 m.

We also modeled the shoreline position and assessed the rate of coastal processes: under the scenario of increasing the lake level to 1903.5 m as a result of full implementation of the relevant law [34]. The resulting flooding would threaten three hotels, five industrial facilities, and 171 single buildings in the coastal zone (Figures 7 and 8). There are approximately 70 km of hard-surfaced roads situated along coasts intensively affected by abrasion. Coastal forests totaling 13.87 km² are at risk of degradation due to active shore erosion.

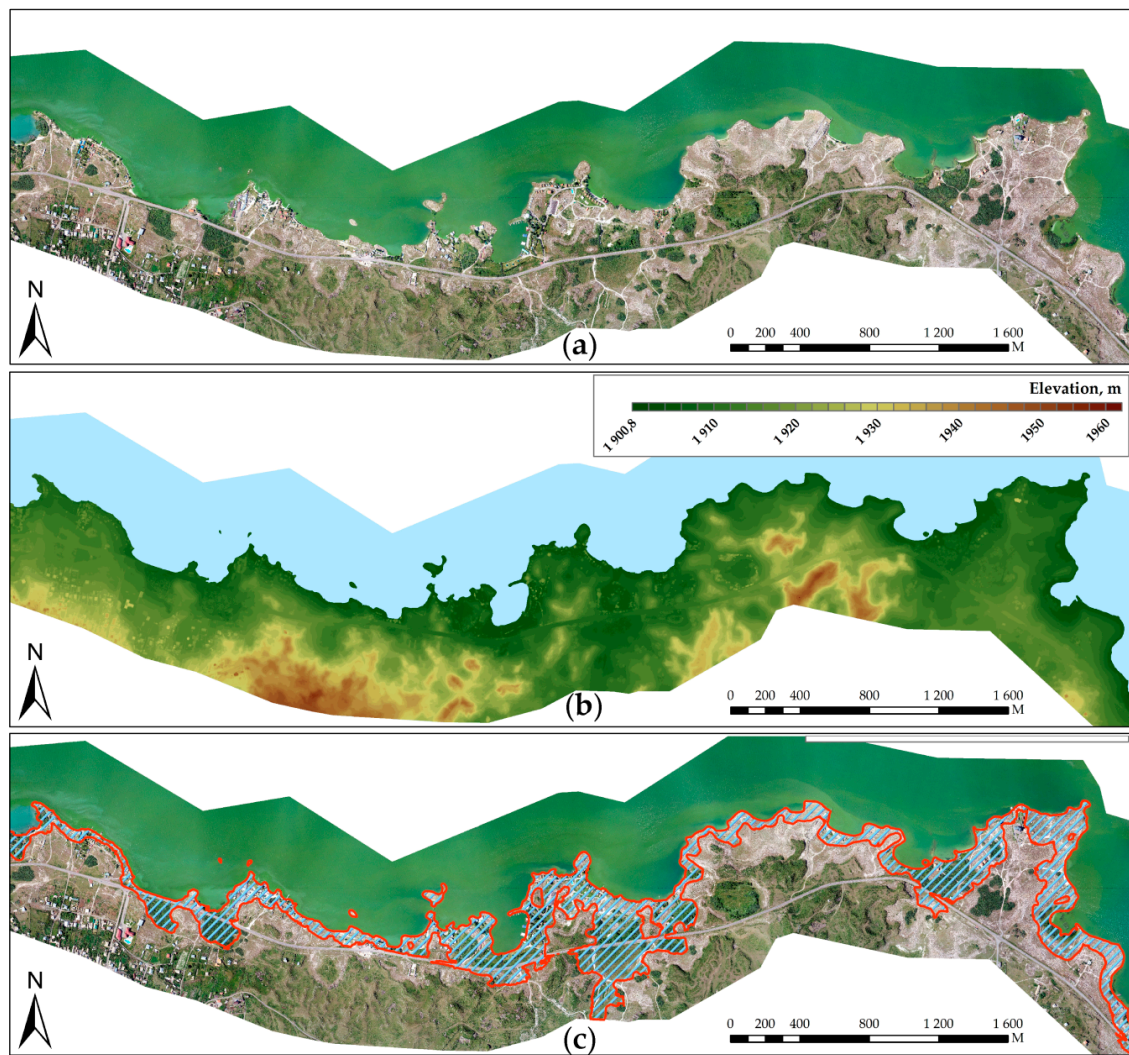


Figure 7. Modelling the submerged areas along the western coasts of Minor Sevan under the scenario of increasing water level: (a) UAV-derived ortho-mosaic, (b) UAV-derived DSM, and (c) areas submerged under the increasing water level up to 1903.5 m.

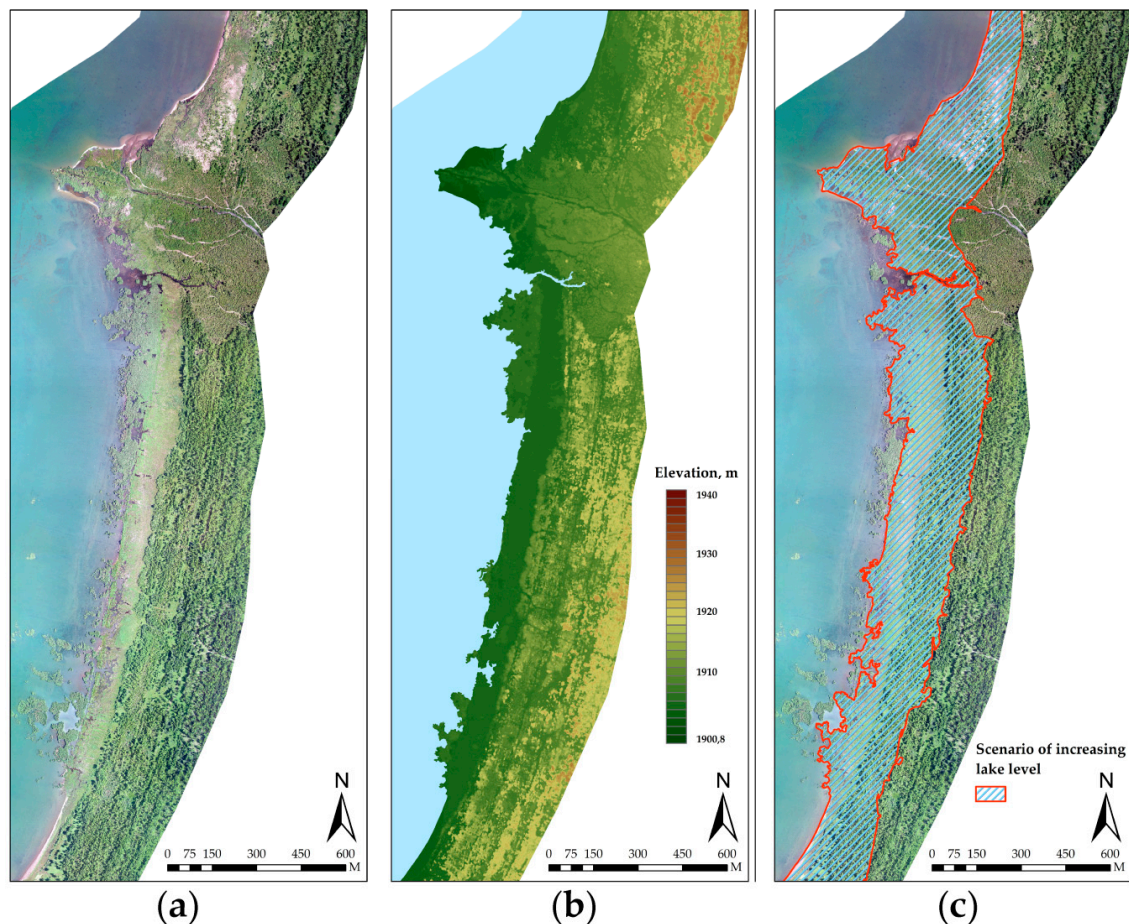


Figure 8. Modelling the submerged areas along the eastern coasts of Major Sevan under the scenario of increasing water level: (a) UAV-derived ortho-mosaic, (b) UAV-derived DSM, and (c) areas submerged under the increasing water level up to 1903.5 m.

3.3. Monitoring of Marsh Shores and Coastal Wetlands

Changes of the water level in Lake Sevan and fluctuations of its shoreline during the past 90 years led to restructuring and areal extension of coastal wetlands [38] with the formation of marsh shores [56], now occupying more than 10% of the entire shoreline, as stated in Section 3.2.

Coastal wetlands of the Norashen Peninsula have an especially high conservation value as breeding grounds of the endemic and rare gull species *Larus armenicus*. The mouths of the Gavaraget, Litchk, Argitchi, and Masrik rivers together with adjacent coastal wetlands as well as the shores of the Noratus and Artanish peninsulas are considered the main breeding sites of rare and valuable fish species and essential waterbird habitats [57]. According to the existing zoning scheme of the Sevan National Park, all these coastal sites and wetlands are classified as strict nature reserves or wildlife sanctuaries [58], but they are now at risk due to changes in hydrological conditions of the shallow waters and water quality [59] as well as overexploitation of their biological resources [57]. Submergence and flooding of coastal habitats lead to active decay of biomass, which intensifies eutrophication and provokes hazardous algal blooms [39]. Only the research of marsh shores and their shoreline positions serves as a basis for assessing the influence of ongoing local hydrological and ecosystem processes upon the quality and state of the aquatic environment in Lake Sevan as a whole.

Although the influence of climate change on water quality fluctuations in Lake Sevan is not entirely understood [37,39,40], abnormally warm conditions during 2018 and 2019 [33] were associated with large and prolonged toxic algal blooms of *Cyanophyta* [40]. For these years, we conducted time series analysis of multi-spectral images (with spatial resolution of 3 m) from PlanetScope constellation

for two sites with marshes and coastal wetlands (Norashen peninsula on Minor Sevan and the eastern part of Major Sevan near the mouth of the Masrik River). It was found that algal blooms began five to seven days earlier in 2019 than in July 2018, which is characterized generally with lower primary production (indicated by moderate values of SABI in surface coastal waters) and shorter duration. In particular, along the coasts of Norashen Peninsula on Minor Sevan, algal blooms were recorded from 4 to 9 July of 2019 and from 9 to 25 July of 2018 (Figure 9). In both 2018 and 2019, blooms initially occurred in coastal waters of the Major Sevan where, according to data from the PlanetScope satellites constellation, the algal films were involved in large vortex structures (Figure 10). UAV-based daytime surveys (operational surveys by PlanetScope satellites are performed at 07:00 to 09:00 local time) made it possible to detect diurnal fluctuations in algal films in close proximity to lacustrine shores, which are most popular and well equipped for summer recreation.

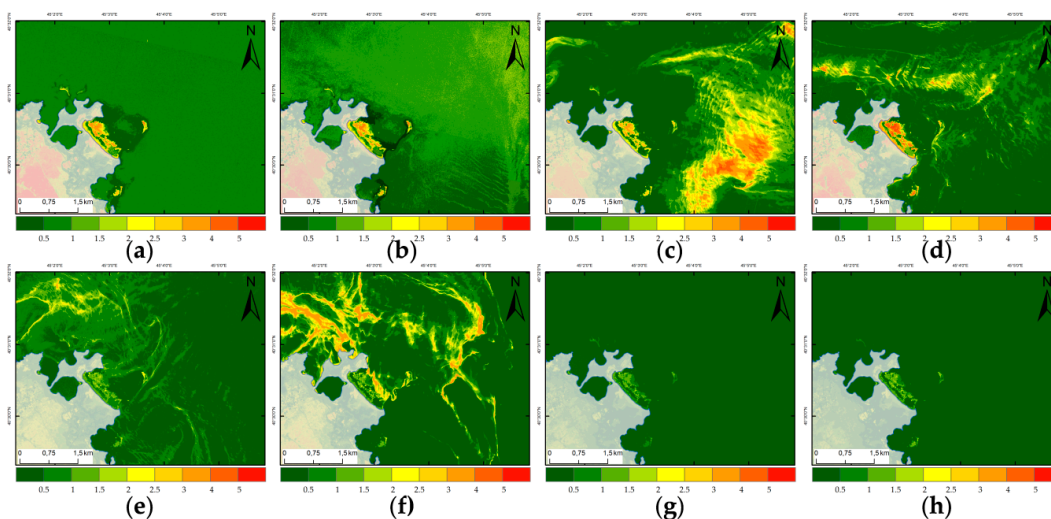


Figure 9. Development of the HAB outbreaks along the western marsh coasts of Minor Sevan, Norashen Peninsula, according to SABI values on 4, 9, 18, and 25 July 2018 (a–d) and on 4, 9, 19, and 22 July 2019 (e–h). Index time series is constructed from multispectral surface reflectance data of PlanetScope [44].

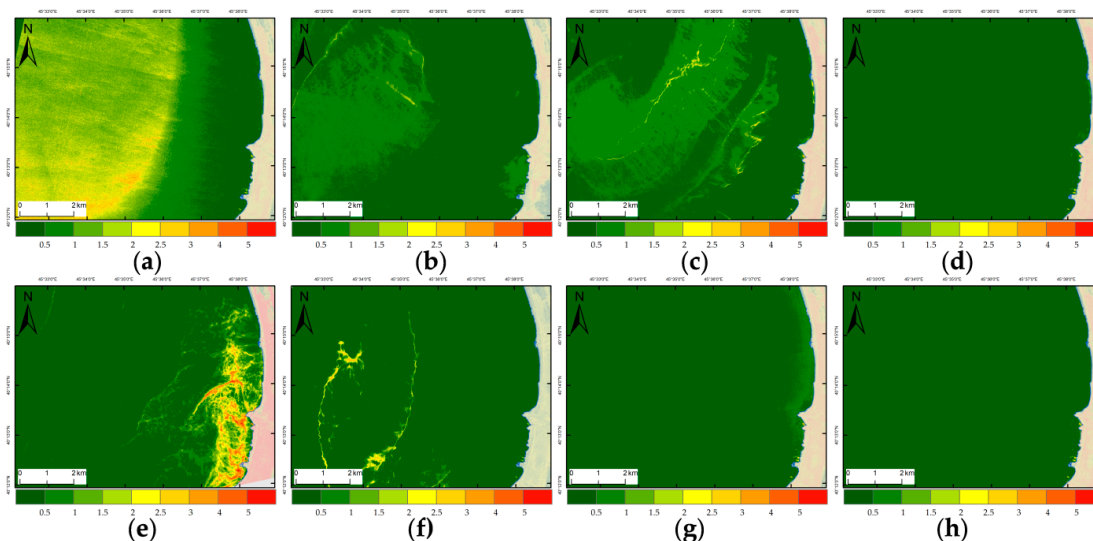


Figure 10. Development of HAB outbreaks along the south-eastern coasts of Major Sevan, near the mouth of Masrik River, according to SABI values on 5, 9, 18, and 24 July 2018 (a–d) and on 2, 9, 19, and 22 July 2019: (e–h) Index time series is constructed from multispectral surface reflectance data of PlanetScope [44].

Thermal surveys of shallow waters and wetlands near the mouth of the Masrik River made it possible to clearly distinguish streams of riverine waters with lower surface temperature, flowing through thick cattail marshes, and using the temperature gradient to identify where it mixed with the lake waters (Figure 11).

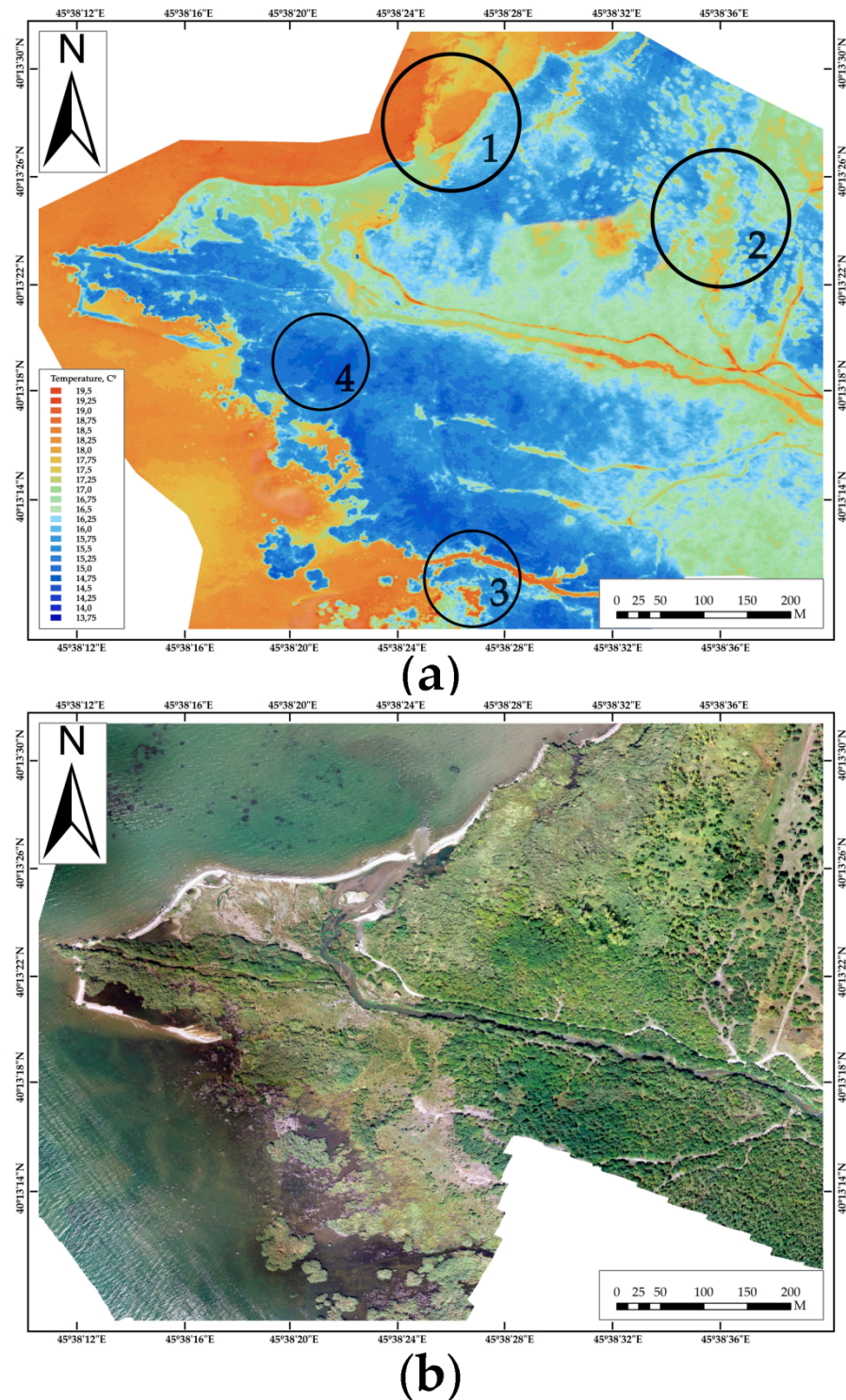


Figure 11. Structure of coastal wetlands in the mouth of Masrik river by thermal (a) and optical (b) UAV imagery. Circles with figures marked by specific thermal signatures of the following objects and phenomena: 1—mixing of riverine and lacustrine waters, 2—living tree vegetation, 3—decay of dead submerged vegetation, and 4—small path of river flow undetected in optical imagery.

This result is well consistent with time series analysis of multispectral high-resolution PlanetScope satellite imagery. Even in a period of intense algal blooming, the area influenced by the mouth of the Masrik River is distinguished by a characteristic plume of turbid surface waters with low primary productivity (according to SABI values spatial distribution, see Figure 10).

4. Discussion

4.1. UAV Surveys as a Part of Multi-Platform Environmental Monitoring of the Lake Sevan Coastal Zone

Water withdrawal for agriculture, runoff from livestock farms, pastures, croplands, fish farms, sewage, wastes from residential areas and industrial units, and heavy recreational loads in a coastal zone are the main drivers of water supply and water quality issues of Lake Sevan. All these human activities pertain to the most important sectors of Armenia's economy. Thus, no measures to reduce their environmental impacts are expected in the near future. Furthermore, within the agrarian Gegharkunik Province, only 56.8% of the total population was economically active in 2018, and improved employment prospects are connected only with agriculture, fisheries (Lake Sevan is the main supplier of fish for the whole country), and recreation [60]. Our large-scale mapping of point and non-point sources of anthropogenic impacts demonstrated that, in a coastal zone and drainage basin of Minor Sevan, the built-up areas and recreational facilities prevailed. Major Sevan is more affected by agricultural runoff from the drainage basin, but its coasts are not so widely-used for organized recreation (Figure 4).

Recreational services are regarded by Armenia's government as one of its main income sources and will, therefore, be promoted in the future. It is possible to reduce the negative impact of tourism only by offering tourism services of higher quality. There are three challenges.

1. Illegal land development;
2. Discharge of untreated sewage water;
3. Environmentally unsound behavior of local people and tourists.

For the area in the study, these challenges are exacerbated by insufficient or absent topical fine-scaled spatial data [42]. As an example, in the course of an inspection organized by the Ministry of Environment in 2020, about 130 cases of illegal economic activity, unauthorized construction, and 150 cases of contractual renting without official registration were identified within the coastal zone of Lake Sevan [58]. Of 300 sites along Lake Sevan shores equipped for recreation and entertainment, only 17 have local wastewater treatment facilities.

Using highly detailed UAV-derived DSMs for two extensive parts of coastal zone, we primarily identified residential buildings, recreational facilities, and fragments of roads within the area of expected flooding under the planned water level rise up to 1903.5 m. Bearing in mind that most of them are not properly documented [42], such acquired results have a high significance for coastal management and cadastral accounting. The identification and large-scale delineation of natural coastal habitats under the risk of waterlogging and submerging is necessary for spatial planning of clearing such sites to prevent the decay of biomass as an additional driver of lake eutrophication.

Agricultural lands, sites for endemic aquaculture, and fish net poaching have undeniable impacts on water quality. However, to date, contribution of such runoff to lake eutrophication and HAB issues have not been well-studied either qualitatively or quantitatively [37,41]. Eutrophication and increasing HAB's outbreaks have clear consequences for bathing, irrigation, water sources for animals, and nutrition for fish, but these issues have not been well-studied [40]. For the time being, toxicity parameters are not included in development plans for the territory around Lake Sevan [42]. Complex use of UAV-derived data and multispectral satellite imagery allowed us to distinguish the spatio-temporal pattern of HABs at a large scale in 2018–2019 specific to both Minor Sevan and Major Sevan.

Under conditions of divergent human-induced changes of the water level, severe and disparate impacts associated with human activities, low efficiency of environmental policies, and a lack for

adequate and detailed spatial data, there is evidently a need to devise and implement a remote sensing system for regular monitoring of the environmental situation in the Lake Sevan coastal zone. Best practices for such monitoring in many coastal environments are based on the use of hierarchic multi-scale and multi-platform approaches, integrating data with differing spatial resolutions and spectral ranges, obtained from various sources with different periodicity [2,6,27,53]. Taking into consideration specific features of the study site and the totality of local environmental problems, the proposed monitoring system could adopt the structure presented in Table 3 with respect to the capabilities of acquiring and processing satellite and UAV data. It should be emphasized that the proposed system relies mainly on open satellite imagery or data, freely accessible through research and educational licenses. Highly detailed optical surveys, which can be performed rapidly by means of compact, low-budget UAVs, play a prominent role in the proposed system. Such surveys can be carried out by personnel of environmental institutions or volunteers without special piloting skills, making it possible to obtain ultra-high resolution data for various territories at very frequent intervals.

Table 3. Proposed multi-platform, multi-scale, and multi-temporal system for environmental remote sensing monitoring of Lake Sevan.

Thematic Task	Spatial Scope (Spatial Resolution)	Periodicity	Platforms
Monitoring land use structure and changes	Drainage basin 10–30 m	Annually	Multi-spectral multi-seasonal satellite data (Landsat 8 OLI, Sentinel-2 MSI)
	Coastal zone 1–3 m	Annually	Annual mosaics of highly detailed satellite imagery
Monitoring pollution point-sources in the coastal zone and their state	Coastal zone (1–3 m, first cm)	Annually and on request	Annual mosaics of highly detailed satellite imagery and on-demand UAV-derived imagery
Monitoring spontaneous littering	Coastal zone outside of developed recreation facilities (better than 0.1 m)	Weekly and on request	Optical surveys from UAV
Monitoring of shore erosion	Infrastructure and communication facilities in the coastal zone and adjacent areas (better than 0.1 m)	Daily and on request	Optical surveys from UAVs
Monitoring the submerged and flooded shores	Waterlogged or submerged coastal habitats (better than 0.1 m)	Weekly and on request	Optical surveys from UAV
	Water body of Lake Sevan, 250–300 m	Daily	Multi-spectral, low-resolution satellite data (Sentinel 3 OLCI, Terra/Aqua MODIS)
Monitoring water quality and environmental state of water bodies	Water body of Lake Sevan, 10–30 m	Once per 3–7 days	Multi-spectral, multi-seasonal satellite data of medium resolution (Landsat 8 OLI, Sentinel-2 MSI)

Table 3. Cont.

Thematic Task	Spatial Scope (Spatial Resolution)	Periodicity	Platforms
	Recreationally developed areas in coastal zone and adjacent waters, nearshore waters around river mouths (3 m)	Daily	Multi-spectral data from PlanetScope microsatellite constellation
	Recreationally developed areas in coastal zone and adjacent waters, nearshore waters around river mouths, coastal wetlands (better than 0.1 m)	In cases of early warning and prompt response up to several times per day, on request	UAV-derived data in the visible, infrared, and thermal bands

4.2. Applications of UAV-Derived Highly Detailed Optical and Thermal Data for Monitoring Coastal Processes

The key findings of conducted UAV-derived multi-temporal data analysis have demonstrated that the currently changing water level of Lake Sevan leads to a rather uneven distribution and intensity of coastal processes along the shoreline. First, the rise in water level entailed activation of destructive shoreline processes, resulting in broader development of erosional coasts. Our calculation of short-term (one to two years) parameters of shoreline at key sites revealed that destruction of shores classified as present-day erosional is highly intensive. The rate of shore erosion exceeds 3.5 m/year in some places such as forested cliffs of Cape Tsovinar along the Major Sevan coast.

The prevailing contemporary coasts along Lake Sevan are accumulative coasts (Table 2). They are mainly submerged due to the present water level rise but show rates of shoreline destruction significantly lower than those of erosional coasts. Some coastal sites display current activity of shore accretion, compensating the water level rise and inducing the broadening coastal areas.

In the formation of present-day coasts, a significant role is played by biogenous factors. Since the man-made forests and shrublands dominated by the area in a coastal zone (especially along the shoreline of Major Sevan), the structural transformation of coastal habitats has led to a high increase of living and dead biomass near the shores. The current degradation of eroded and submerged forested shores in some key sites (Norashen Peninsula, sites along Major Sevan coasts) is so heavy that it became impossible to detect accurately shoreline positions, even with the help of ultra-high spatial resolution UAV imagery.

As a result of conducted highly detailed optical and thermal UAV surveys for key coastal sites, we propose monitoring of marsh shores and coastal wetlands by the following findings.

1. Research in the habitat structure and the state of vegetation cover. UAV survey data can identify the types of vegetation communities not only through their species composition but also through indirect indicators in the form of specific plants, which indicate the degree of water abundance in those cases when it is impossible to interpret ground features beneath thick vegetation cover. UAV-based optical survey data allow reliable interpretation of vegetation species' composition and habitat types, while thermal surveys additionally enable identifying the areas of different water abundance and determining species structure, spatial patterns, and the ecological status of forest plantations, shrubland, and grassland from their thermal images.
2. The monitoring of processes related to decay of macrobiota. The processes of biota decomposition at flooded coastal sites lead to heat emissions and irreversible chemical reactions. These exothermic reactions in coastal waters can contribute to eutrophication and, combined with high aerial temperatures especially during the spring–summer period, can also exacerbate algal blooms in surface waters. Locations of vegetation decay were identified from UAV-derived thermal surveys

(Figure 11). Some uncertainties remain, however, regarding the interpretation of nadir thermal images as well as living and decaying vegetation on hillocks within marshes. Oblique aerial thermal and optical survey seems to be the only means of resolving this problem.

3. Monitoring of the hydrothermal regime. Research into hydrothermal regimes and representation of processes related to mixing of lagoon, marsh, or river waters with the lake waters are important constituents of water quality monitoring. UAV-based thermal images identified the main mixing areas of waters flowing out of marsh swamps and lagoons (Figure 11). In the coastal zone of the Norashen Peninsula, which is an extremely dynamic area among all key study sites, the thermal survey results helped to elucidate the complex structural dynamic system of nearshore waters, semi-closed and closed lagoons, foreshores, and marsh swamps of different types (reed and cattail species). Such a landscape is unique for Lake Sevan shores. The temperature gradient at different habitats on the Norashen peninsula manifested not only in UAV-based thermal surveys but also tested by hydrobiological studies that revealed a distinct spatial pattern of local communities of zoobenthos [61].

4.3. Prospective Applications of UAV Surveys in the System of Environmental Coastal Monitoring

It is impossible to resolve problems of prompt thematic mapping and comprehensive monitoring without the use of UAVs. This is due to the opportunities to obtain spatial data of extremely high resolution (up to sub-centimeters) and to perform repeated surveys. UAV-derived ultra-high resolution data cannot always be substituted by detailed satellite imagery because the sub-meter spatial resolution of even multi-spectral and hyper-spectral data does not allow identification of specific objects and features in coastal environments under some thematic tasks. The diurnal timetable of surveys from orbital satellites or satellite constellations is also poorly suited for monitoring objects that change their parameters within a day or even hours. Issues of large-scale and accurate detection of shoreline position are also a task solely for UAVs and other unmanned aerial platforms.

Those problems, which can and should be resolved solely through the use of UAVs in the sphere of shore and shore processes research, can be clearly arranged into two categories, namely: prompt responses and consistent observation within a general framework of regular monitoring. In turn, these blocks can be sub-divided according to types of survey equipment and minimal spatial resolution necessary for resolving specific thematic tasks for identifying the main processes having a negative environmental impact on coastal areas and waters.

In case of the Lake Sevan, a special task to be resolved using the only ultra-high resolution UAV-data was the detection of point sources of water pollution. This task was divided into three sections with each utilizing data of different spatial resolution (obtained from UAV surveys at different flight levels) for:

1. Detection of small domestic wastes and plastics. To resolve this task, UAV-derived data obtained at very low survey altitudes (100 m and less) should be used as the recognition of such features is possible only with imagery of sub-decimeter spatial resolution. The surveys identified construction waste in coastal zones as well as clusters of abandoned fishing nets in waters. These nets are traces of illegal, uncontrolled fishing and often become places of active organic decay of macro-biota (including both fish and bird fauna caught in them).
2. Monitoring of camping sites or temporary stay by tourists as sources of coastal littering. Tourist activities along the southern and eastern coasts of Lake Sevan have generated spontaneous and uncontrolled miniature landfills that are not included in waste disposal systems of settlements and static tourist accommodation sites.
3. Detection of points of illegal sewage discharge into the lake. Some recreational housing in the coastal zone comprises temporary structures lacking adequate sewage treatment system, often with all waste waters discharged by the pipeline directly into the lake.

At present, the most promising tasks are those that are resolved with the help of UAV-based multi-spectral and hyper-spectral data, including thermal imagery. The analysis of the state and structure of vegetation in nearshore waters and of submerged aquatic vegetation (phyto-indication using multi-spectral and hyper-spectral UAV-derived data) can be already considered as a specific thematic branch of coastal monitoring [15–17,20].

In terms of tasks for regularly monitoring anthropogenic impacts on coastal ecosystems and waters and assessing the effectiveness of conservation and environmental measures, the thermal survey may move to the fore. Discharge of industrial and domestic wastewaters can be especially well detected in the thermal spectral range. It is possible to use such thermal UAV images as evidences of environmental violations in case they are supplemented with data acquired simultaneously or in near-time from field hydro-chemical sampling or ground hyper-spectral remote sensing.

Prospects for the use of optical UAV-derived data are connected not only with simple recording of violations of water and environmental management rules. Acquisition from ultra-low-height UAV optical surveys and thematic application of such a derived product of digital aerial photogrammetry as photogrammetric dense point clouds and ultra-highly detailed digital surface models (DSMs) raises UAVs to an important basic level within multi-platform monitoring systems.

Nevertheless, the cost-efficiencies and time-efficiencies of UAV surveys in coastal areas, the quality of acquired data, and their adequacy for studying highly dynamic objects and processes strongly depend on specific conditions formed in water environments [28]. Acquisition and processing UAV-based data in the course of coastal environmental studies involves some difficulties and restrictions unrelated to survey equipment and principally typical of remote sensing of water bodies: glints, shadows, surface waves, wind speed, and so on.

Rapidly changing conditions of irradiance and water transparency are the key limitations of UAV surveys due to the rather long time required to survey even small areas. Consequently, it is critically important to develop and apply special survey techniques ad hoc, taking into account the peculiarities and phenology of objects and sites in study, and to select appropriate flight times carefully to coincide with optimal meteorological and hydrological conditions, especially for repeated multi-temporal UAV-based studies.

5. Conclusions

The main objective of our study was to demonstrate the main thematic applications of highly-detailed remote sensing data in visible and thermal spectra, obtained as a result of repeated surveys from small UAVs, in the integral system of prompt and regular monitoring of highly dynamic and vulnerable coastal zone of Lake Sevan under diverse anthropogenic impacts and an artificially changing water level. We have elaborated and tested several techniques and protocols of surveys depending on thematic tasks: flights at different heights and in different seasons. The advantage of thermal surveys above optical ones is more accurate identification of coastal wetlands' state and structure. Thermal UAV surveys can be considered as a prospective technology for rapid detection of illegal sewage as well as dead biomass in degraded and submerged habitats.

Our results have shown a very uneven character of anthropogenic impacts in coastal ecosystems by type and level along the shorelines of Minor Sevan and Major Sevan. Resulting from low environmental responsibility of local people and tourists, such environmental violations as illegal land development, direct discharge of raw sewage, fish poaching, and unsound practices of aquaculture, extensive spontaneous clumping of anthropogenic litter along the coasts should be traced and resolved by means of UAV-derived multi-temporal data with ultra-high spatial resolution.

As a result of multi-temporal UAV data analysis, we found out that the high rate of shore erosion (more than 3.5 m per year in some places) and rapid degradation of waterlogged or submerged habitats with decaying biomass promote eutrophication and strong algal blooms. The more vulnerable present-day coastal types with endangered habitats are erosional and marsh coasts, accounting for 28.1% and 10.1%, respectively, of the total shoreline of Lake Sevan. The water rises to 1903.5 m by 2030,

as intended by national legislation can lead, according to our large-scale mapping and spatial analysis, to the complete flooding of road sections, important recreational facilities, and valuable forested areas along the Sevan coasts.

Under the definite advantages of UAV data for specific tasks at the large-scale level and their flexibility of operative or on request acquisition, the UAV-based environmental coastal monitoring of complex and highly dynamic area should become a necessary intermediary between field measurements and satellite RS data in a multi-scaled, multi-temporal, and multi-platform integral scheme for monitoring the coastal zone and water body of the whole Lake Sevan under unprecedented changes in its water level and associated environmental issues and challenges. Approaches and findings presented in this paper can also be implemented for environmental monitoring and coastal management of high-mountainous large lakes or reservoirs in regions with limited water resources.

Author Contributions: Conceptualization, A.M. and N.T. Methodology, A.M. and A.K. UAV data acquisition and software, A.M. and P.K. Validation, N.T., N.A., P.K., S.A., and A.N. Formal analysis, N.T. and N.A. Data curation, A.M. Writing—original draft preparation, A.M., N.T., N.A., A.K., S.A. and A.N. Writing—review and editing, A.M., N.T. and A.K. Visualization, A.M., N.T., and P.K. All authors have read and agreed to the published version of the manuscript.

Funding: This work was supported by the State Committee of Science (SCS) of the Ministry of Science, Education, Culture and Sport of Armenia, and Russian Foundation for Basic Research (RFBR) in the frames of joint research project SCS 18RF-140 and RFBR 18-55-05015 (field studies and UAV surveys in 2018–2019). Additional support was provided by the Institute of Geography, Russian Academy of Sciences, State Assignment number AAAA-A19-119022190168-8.

Acknowledgments: The authors are grateful to Dave Morris who did the proof-reading of the text as well as to the four anonymous reviewers for their valuable comments on the previous versions of the manuscript. We would like to thank Garegin Tepanosyan and Vahagn Muradyan (Centre for Ecological-Noosphere Studies) for their help and support with our fieldworks in Armenia, and Alexander Khropov (Institute of Geography, Russian Academy of Sciences) for his advice on English translation of this paper and standardization of geographical names. We also thank Planet Team's research and education program for providing granted access to PlanetScope imagery.

Conflicts of Interest: The authors declare no conflict of interest.

References

1. Klemas, V. Coastal and Environmental Remote Sensing from Unmanned Aerial Vehicles: An Overview. *J. Coast. Res.* **2015**, *315*, 1260–1267. [[CrossRef](#)]
2. Kislik, C.; Dronova, I.; Kelly, M. UAVs in Support of Algal Bloom Research: A Review of Current Applications and Future Opportunities. *Drones* **2018**, *2*, 35. [[CrossRef](#)]
3. Green, D.R.; Hagon, J.J.; Gómez, C.; Gregory, B.J. Chapter 21—Using low-cost UAVs for environmental monitoring, mapping, and modelling: Examples from the coastal zone. In *Coastal Management*; Krishnamurthy, R.R., Jonathan, M.P., Srinivasalu, S., Glaeser, B., Eds.; Academic Press: New York, NY, USA, 2019; pp. 465–501. ISBN 978-0-12-810473-6.
4. Tmušić, G.; Manfreda, S.; Aasen, H.; James, M.R.; Gonçalves, G.; Ben-Dor, E.; Brook, A.; Polinova, M.; Arranz, J.J.; Mészáros, J.; et al. Current Practices in UAS-based Environmental Monitoring. *Remote Sens.* **2020**, *12*, 1001. [[CrossRef](#)]
5. Becker, R.H.; Sayers, M.; Dehm, D.; Shuchman, R.; Quintero, K.; Bosse, K.; Sawtell, R. Unmanned aerial system based spectroradiometer for monitoring harmful algal blooms: A new paradigm in water quality monitoring. *J. Great Lakes Res.* **2019**, *45*, 444–453. [[CrossRef](#)]
6. Cillero Castro, C.; Domínguez Gómez, J.A.; Delgado Martín, J.; Hinojo Sánchez, B.A.; Cereijo Arango, J.L.; Cheda Tuya, F.A.; Díaz-Varela, R. An UAV and Satellite Multispectral Data Approach to Monitor Water Quality in Small Reservoirs. *Remote Sens.* **2020**, *12*, 1514. [[CrossRef](#)]
7. Gonçalves, J.A.; Henriques, R. UAV photogrammetry for topographic monitoring of coastal areas. *ISPRS J. Photogramm. Remote Sens.* **2015**, *104*, 101–111. [[CrossRef](#)]
8. Lowe, M.K.; Adnan, F.A.F.; Hamylton, S.M.; Carvalho, R.C.; Woodroffe, C.D. Assessing Reef-Island Shoreline Change Using UAV-Derived Orthomosaics and Digital Surface Models. *Drones* **2019**, *3*, 44. [[CrossRef](#)]

9. Burdziakowski, P.; Specht, C.; Dąbrowski, P.; Specht, M.; Lewicka, O.; Makar, A. Using UAV Photogrammetry to Analyse Changes in the Coastal Zone Based on the Sopot Tombolo (Salient) Measurement Project. *Sensors* **2020**, *20*, 4000. [\[CrossRef\]](#)
10. Zanutta, A.; Lambertini, A.; Vittuari, L. UAV Photogrammetry and Ground Surveys as a Mapping Tool for Quickly Monitoring Shoreline and Beach Changes. *J. Mar. Sci. Eng.* **2020**, *8*, 52. [\[CrossRef\]](#)
11. Alvarez, L.V.; Moreno, H.A.; Segales, A.R.; Pham, T.G.; Pillar-Little, E.A.; Chilson, P.B. Merging Unmanned Aerial Systems (UAS) Imagery and Echo Soundings with an Adaptive Sampling Technique for Bathymetric Surveys. *Remote Sens.* **2018**, *10*, 1362. [\[CrossRef\]](#)
12. Esposito, G.; Salvini, R.; Matano, F.; Sacchi, M.; Danzi, M.; Somma, R.; Troise, C. Multitemporal Monitoring of a Coastal Landslide Through SfM-Derived Point Cloud Comparison. *Photogramm. Rec.* **2017**, *32*, 459–479. [\[CrossRef\]](#)
13. Jaud, M.; Delacourt, C.; Le Dantec, N.; Allemand, P.; Ammann, J.; Grandjean, P.; Nouaille, H.; Prunier, C.; Cuq, V.; Augereau, E.; et al. Diachronic UAV Photogrammetry of a Sandy Beach in Brittany (France) for a Long-Term Coastal Observatory. *ISPRS Int. J. Geo inf.* **2019**, *8*, 267. [\[CrossRef\]](#)
14. Gómez-Gutiérrez, Á.; Gonçalves, G.R. Surveying Coastal Cliffs using Two UAV Platforms (Multirotor and Fixed-Wing) and Three Different Approaches for the Estimation of Volumetric Changes. *Int. J. Remote Sens.* **2020**, 1–33. [\[CrossRef\]](#)
15. Corti Meneses, N.; Brunner, F.; Baier, S.; Geist, J.; Schneider, T. Quantification of Extent, Density, and Status of Aquatic Reed Beds using Point Clouds Derived from UAV–RGB Imagery. *Remote Sens.* **2018**, *10*, 1869. [\[CrossRef\]](#)
16. Duffy, J.P.; Pratt, L.; Anderson, K.; Land, P.E.; Shutler, J.D. Spatial Assessment of Intertidal Seagrass Meadows using Optical Imaging Systems and a Lightweight Drone. *Estuar. Coast. Shelf Sci.* **2018**, *200*, 169–180. [\[CrossRef\]](#)
17. Ventura, D.; Bonifazi, A.; Gravina, M.F.; Belluscio, A.; Ardizzone, G. Mapping and Classification of Ecologically Sensitive Marine Habitats using Unmanned Aerial Vehicle (UAV) Imagery and Object-Based Image Analysis (OBIA). *Remote Sens.* **2018**, *10*, 1331. [\[CrossRef\]](#)
18. Nahirnick, N.K.; Reshitnyk, L.; Campbell, M.; Hessing-Lewis, M.; Costa, M.; Yakimishyn, J.; Lee, L. Mapping with Confidence; Delineating Seagrass Habitats using Unoccupied Aerial Systems (UAS). *Remote Sens. Ecol. Conserv.* **2019**, *5*, 121–135. [\[CrossRef\]](#)
19. Gray, P.C.; Ridge, J.T.; Poulin, S.K.; Seymour, A.C.; Schwantes, A.M.; Swenson, J.J.; Johnston, D.W. Integrating Drone Imagery into High Resolution Satellite Remote Sensing Assessments of Estuarine Environments. *Remote Sens.* **2018**, *10*, 1257. [\[CrossRef\]](#)
20. Doughty, C.L.; Cavanaugh, K.C. Mapping Coastal Wetland Biomass from High Resolution Unmanned Aerial Vehicle (UAV) Imagery. *Remote Sens.* **2019**, *11*, 540. [\[CrossRef\]](#)
21. Kalacska, M.; Chmura, G.L.; Lucanus, O.; Bérubé, D.; Arroyo-Mora, J.P. Structure from Motion Will Revolutionize Analyses of Tidal Wetland Landscapes. *Remote Sens. Environ.* **2017**, *199*, 14–24. [\[CrossRef\]](#)
22. Gonçalves, G.; Andriolo, U.; Pinto, L.; Bessa, F. Mapping marine litter using UAS on a beach-dune system: A multidisciplinary approach. *Sci. Total Environ.* **2020**, *706*, 135742. [\[CrossRef\]](#) [\[PubMed\]](#)
23. Hengstmann, E.; Fischer, E.K. Anthropogenic Litter in Freshwater Environments—Study on Lake Beaches Evaluating Marine Guidelines and Aerial Imaging. *Environ. Res.* **2020**, *189*, 109945. [\[CrossRef\]](#) [\[PubMed\]](#)
24. Merlino, S.; Paterni, M.; Berton, A.; Massetti, L. Unmanned Aerial Vehicles for Debris Survey in Coastal Areas: Long-Term Monitoring Programme to Study Spatial and Temporal Accumulation of the Dynamics of Beached Marine Litter. *Remote Sens.* **2020**, *12*, 1260. [\[CrossRef\]](#)
25. Ansari, A.A.; Gill, S.S.; Khan, F.A. Eutrophication: Threat to Aquatic Ecosystems. In *Eutrophication: Causes, Consequences and Control*; Ansari, A.A., Singh Gill, S., Lanza, G.R., Rast, W., Eds.; Springer: Dordrecht, The Netherlands, 2010; pp. 143–170. ISBN 978-90-481-9624-1.
26. Wu, D.; Li, R.; Zhang, F.; Liu, J. A Review on Drone-based Harmful Algae Blooms Monitoring. *Environ. Monit. Assess.* **2019**, *191*. [\[CrossRef\]](#)
27. Xing, Q.; An, D.; Zheng, X.; Wei, Z.; Wang, X.; Li, L.; Tian, L.; Chen, J. Monitoring Seaweed Aquaculture in the Yellow Sea with Multiple Sensors for Managing the Disaster of Macroalgal Blooms. *Remote Sens. Environ.* **2019**, *231*, 111279. [\[CrossRef\]](#)
28. Doukari, M.; Batsaris, M.; Papakonstantinou, A.; Topouzelis, K. A Protocol for Aerial Survey in Coastal Areas using UAS. *Remote Sens.* **2019**, *11*, 1913. [\[CrossRef\]](#)

29. Turner, I.; Harley, M.; Drummond, C. UAVs for Coastal Surveying. *Coast. Eng. J.* **2016**, *114*, 19–24. [CrossRef]
30. Davydov, V.K. *Vodnyj Balans Oзера Sevan (The Water Balance of Lake Sevan)*; Materials on Study of Lake Sevan and Its Basin; Gydrometizdat: Leningrad, Russia, 1938; Volume VI, pp. 12–82. (In Russian)
31. Babayan, A.; Hakobyan, S.; Jenderedjian, K.; Muradyan, S.; Voskanov, M. *Lake Sevan: Experience and Lessons Learned Brief*; Lake basin management initiative; International Lake Environment Committee Foundation: Kusatsu, Japan, 2006; pp. 1–28.
32. The Republic of Armenia; Ministry of Emergency Situations. *Hydrological Regime of Lake Sevan*; Service of the Hydrometeorology and Active Influence on Atmospheric Phenomena; Ministry of Emergency Situations RA: Yerevan, Armenia, 2017; pp. 1–13. (In Armenian)
33. The Republic of Armenia; Ministry of Emergency Situations. Five-Day Weather Forecast Data for Armenia. Rivers, Lakes and Reservoirs. Data on SEVAN. Available online: <http://mes.am/hy/weather/item/2020/08/11/1313> (accessed on 24 August 2020).
34. The Republic of Armenia. Law on Measures for Restoration, Maintenance, Reproduction and Use of Lake Sevan Ecosystem. Available online: <http://www.parliament.am/legislation.php?sel=show&ID=1676&lang=arm&enc=utf8> (accessed on 24 August 2020). (In Armenian)
35. The Republic of Armenia; Ministry of Urban Development. Guidelines on Territorial Activities Coordination Parallel to Raising the Water Level of Lake Sevan. Available online: http://mud.am/lows/files/SEVAN_JRACACKUM_TEXT_HRAMAN_HASTATVAC.pdf (accessed on 24 August 2020). (In Armenian)
36. Danielyan, K.; Gabrielyan, B.; Minasyan, S.; Chilingaryan, L.; Melkonyan, H.; Karakhanyan, A.; Tozalakyan, P.; Vanyan, A.; Pirumyan, G.; Ghukasyan, E.; et al. *Integrated Assessment of the Lake Sevan Environmental Conditions (GEO—Lake Sevan)*; The Association “For Sustainable Human Development”/UNEP National Committee; Yerevan, Armenia, 2011; pp. 29–69. (In Russian)
37. Vardanian, T. On Some Issues of the Anthropogenic Transformation of Water Ecosystems (Case Study of Lake Sevan). In *National Security and Human Health Implications of Climate Change*; NATO Science for Peace and Security Series C: Environmental Security; Springer: Dordrecht, The Netherlands, 2012; pp. 325–336. ISBN 978-94-007-2429-7.
38. Pavlov, D.S.; Poddubnyi, S.A.; Gabrielyan, B.K.; Krylov, A.V. (Eds.) *Ecology of Lake Sevan During the Period of Water Level Rise. The Results of Russian-Armenian Biological Expedition for Hydroecological Survey of Lake Sevan (Armenia) (2005–2009)*; Nauka DNC: Makhachkala, Russia, 2010; pp. 28–50. ISBN 978-5-94434-162-4. (In Russian)
39. Sakharova, E.G.; Krylov, A.V.; Sabitova, R.Z.; Tsvetkov, A.I.; Gambaryan, L.R.; Mamyan, A.S.; Gabrielyan, B.K.; Hayrapetyan, A.H.; Khachikyan, T.G. Horizontal and Vertical Distribution of Phytoplankton in the Alpine Lake Sevan (Armenia) during the Summer Cyanoprokaryota bloom. *Contemp. Probl. Ecol.* **2020**, *13*, 60–70. [CrossRef]
40. Gevorgyan, G.; Rinke, K.; Schultze, M.; Mamyan, A.; Kuzmin, A.; Belykh, O.; Sorokovikova, E.; Hayrapetyan, A.; Hovsepyan, A.; Khachikyan, T.; et al. First Report about Toxic Cyanobacterial Bloom Occurrence in Lake Sevan, Armenia. *Int. Rev. Hydrobiol.* **2020**. [CrossRef]
41. Wilkinson, I.P. Lake Sevan: Evolution, biotic variability and ecological degradation. In *Large Asian Lakes in a Changing World*; Mischke, S., Ed.; Springer International Publishing: Cham, Switzerland, 2020; pp. 35–63. ISBN 978-3-030-42253-0.
42. Margaryan, L.; Yeritsyan, H.; Arakelyan, A.; Martirosyan, A.; Avagyan, A.; Tarasyan, N.; Uloyan, H.; Sargsyan, L.; Nersisyan, A. *Development of Draft River Basin Management Plan for Sevan River Basin District in Armenia: Phase 2*; European Union Water Initiative Plus for Eastern Partnership Countries (EUWI+): Results 2 and 3; EU Member State Consortium: Vienna, Austria, 2020; pp. 1–51.
43. Agisoft Metashape User Manual: Professional Edition, Version 1.6. Available online: https://www.agisoft.com/pdf/metashape-pro_1_6_en.pdf (accessed on 23 August 2020).
44. Planet Labs Inc.; Planet Team. *Application Program Interface. Space for Life on Earth*; San Francisco, CA, USA, 2017. Available online: <https://api.planet.com> (accessed on 24 August 2020).
45. Planet Labs Inc. Planet Surface Reflectance Product. Available online: https://assets.planet.com/marketing/PDF/Planet_Surface_Reflectance_Technical_White_Paper.pdf (accessed on 12 November 2020).
46. Alawadi, F. Detection of Surface Algal Blooms using the Newly Developed Algorithm Surface Algal Bloom Index (SABI). In *Proceedings of the SPIE Remote Sensing of the Ocean, Sea Ice, and Large Water Regions 2010*, International Society for Optics and Photonics, Toulouse, France, 18 October 2010; Volume 7825, p. 782506.

47. Gade, R.; Moeslund, T.B. Thermal Cameras and Applications: A Survey. *Mach. Vision Appl.* **2014**, *25*, 245–262. [CrossRef]
48. Helgesen, H.H.; Leira, F.S.; Bryne, T.H.; Albrektsen, S.M.; Johansen, T.A. Real-Time Georeferencing of Thermal Images using Small Fixed-Wing UAVs in Maritime Environments. *ISPRS J. Photogramm. Remote Sens.* **2019**, *154*, 84–97. [CrossRef]
49. Sledz, A.; Unger, J.; Heipke, C. Thermal IR imaging: Image quality and orthophoto generation. In Proceedings of the ISPRS—International Archives of the Photogrammetry, Remote Sensing and Spatial Information Sciences; Mid-Term Symposium “Innovative Sensing – From Sensors to Methods and Applications”, Karlsruhe, Germany, 10–12 October 2018; Copernicus GmbH: Göttingen, Germany, 2018; Volume XLII–1, pp. 413–420.
50. Lewis, A.; Hilley, G.E.; Lewicki, J.L. Integrated Thermal Infrared Imaging and Structure-from-Motion Photogrammetry to Map Apparent Temperature and Radiant Hydrothermal Heat Flux at Mammoth Mountain, CA, USA. *J. Volcanol. Geoth. Res.* **2015**, *303*, 16–24. [CrossRef]
51. Min, D.; Zhilin, L.; Xiaoyong, C. Extended Hausdorff distance for spatial objects in GIS. *Int. J. Geogr. Inf. Sci.* **2007**, *21*, 459–475. [CrossRef]
52. Shao, F.; Cai, S.; Gu, J. A modified Hausdorff distance based algorithm for 2-dimensional spatial trajectory matching. In Proceedings of the 2010 5th International Conference on Computer Science Education, Hefei, China, 24–27 August 2010; pp. 166–172. [CrossRef]
53. Rossiter, T.; Furey, T.; McCarthy, T.; Stengel, D.B. Application of Multiplatform, Multispectral Remote Sensors for Mapping Intertidal Macroalgae: A Comparative Approach. *Aquat. Conserv. Mar. Freshw. Ecosyst* **2020**. [CrossRef]
54. Leont’ev, O.K. *Geomorfologiya Morskih Beregov i Dna (Geomorphology of the Sea Coasts and Bottom)*; Izdatel’stvo Moskovskogo Universiteta: Moscow, Russia, 1955; pp. 1–377. (In Russian)
55. Zenkovich, V.P. *Osnovy Ucheniya o Razviti Morskikh Beregov (Fundamentals of the Theory on Marine Coast Development)*; Izd-vo Akademii Nauk SSSR: Moscow, Russia, 1962; pp. 1–740. (In Russian)
56. Hovsepyan, A.; Tepanosyan, G.; Muradyan, V.; Asmaryan, S.; Medvedev, A.; Koshkarev, A. Lake Sevan Shoreline Change Assessment using Multi-Temporal Landsat Images. *Geogr. Environ. Sustain.* **2019**, *12*, 212–229. [CrossRef]
57. Ramsar Sites Information Service. Lake Sevan. Available online: <https://rsis Ramsar.org/ris/620> (accessed on 23 August 2020).
58. The Republic of Armenia; Ministry of Nature Protection. Sevan National Park (SNCO)—Territorial-Functional Areas. Available online: <http://sevanpark.am/en/category/about-territory/territorial-functional-areas/> (accessed on 23 August 2020).
59. BirdLife International. Important Bird Areas Factsheet: Lake Sevan and Environs. Available online: <http://datazone.birdlife.org/site/factsheet/lake-sevan-and-environs-iba-armenia/details> (accessed on 23 August 2020).
60. The Republic of Armenia; Statistical Committee. ArmStatBank Database. RA Gegharkunik Marz in Figures. 2019. Available online: <https://www.armstat.am/en/?nid=771> (accessed on 25 August 2020). (In Armenian)
61. Potyutko, O.M.; Kandyba, I.V.; Medvedev, A.A. Ecological and Faunistic Characteristic of the Zooperiphyton of the Contact Zone of Lake Sevan (Armenia). *Russ. J. Zool.* **2020**, *99*, in press.

Publisher’s Note: MDPI stays neutral with regard to jurisdictional claims in published maps and institutional affiliations.



© 2020 by the authors. Licensee MDPI, Basel, Switzerland. This article is an open access article distributed under the terms and conditions of the Creative Commons Attribution (CC BY) license (<http://creativecommons.org/licenses/by/4.0/>).